Ultrasonics - Sonochemistry 51 (2019) 214–222

Contents lists available at ScienceDirect

Ultrasonics - Sonochemistry

journal homepage: www.elsevier.com/locate/ultson

Ultrasonic assisted ultrafiltration process for emulsification of oil field produced water treatment

Augustine Agi[a], Radzuan Junin[a,b,*], Amr Yahya Mohd Alqatta[a], Afeez Gbadamosi[a], Asma Yahya[a], Azza Abbas[a]

[a] Department of Petroleum Engineering, School of Chemical and Energy Engineering, Faculty of Engineering, Universiti Teknologi Malaysia, 81310 Johor Bahru, Malaysia
[b] Institute for Oil and Gas, Universiti Teknologi Malaysia, 81310 Johor Bahru, Malaysia

ARTICLE INFO

Keywords:
Ultrasonic
Ultrafiltration
Cavitation
Membrane flux
Oil-in-water emulsion
Brownian motion

ABSTRACT

Ultrafiltration has been proven to be very effective in the treatment of oil-in-water emulsions, since no chemical additives are required. However, ultrafiltration has its limitations, the main limits are concentration polarization resulting to permeate flux decline with time. Adsorption, accumulation of oil and particles on the membrane surface which causes fouling of the membrane. Studies have shown that the ultrasonic is effective in cleaning of fouled membrane and enhancing membrane filtration performance. But the effectiveness also, depends on the selection of appropriate membrane material, membrane geometry, ultrasonic module design, operational and processing condition. In this study, a hollow and flat-sheet polyurethane (PU) membranes synthesized with different additives and solvent were used and their performance evaluated with oil-in-water emulsion. The steady-state permeate flux and the rejection of oil in percentage (%) at two different modes were determined. A dry/wet spinning technique was used to fabricate the flat-sheet and hollow fibre membrane (HFMs) using Polyethersulfone (PES) polymer base, Polyvinylpyrrolidone (PVP) additive and N, N-Dimethylacetamide (DMAc) solvent. Ultrasonic assisted cross-flow ultrafiltration module was built to avoid loss of ultrasonic to the surrounding. The polyurethane (PU) was synthesized by polymerization and sulphonation to have an anionic group (–OH; –COOH; and –SO_3H) on the membrane surface. Changes in morphological properties of the membrane had a significant effect on the permeate flow rate and oil removal. Generation of cavitation and Brownian motion by the ultrasonic were the dominant mechanisms responsible for ultrafiltration by cracking the cake layers and reducing concentration polarization at the membrane surface. The percentage of oil after ultrafiltration process with ultrasonic is about 90% compared to 49% without ultrasonic. Ultrasonic is effective in enhancing the membrane permeate flux and controlling membrane fouling.

1. Introduction

During oil production, the ratio of produced water can exceed oil production while still in the economic life of a production field [1]. As the oil and gas reach maturity, the amount of produced water keeps increasing and can account for about 98% of the produced fluid in an oil field [2]. Produced water is composed mainly of oil and grease dissolved formation minerals, production chemicals, dissolved gases, produced solid matters and sands (oil emulsion droplet, formation minerals and toxicants) [3,4]. Improper management of this fluid can cause severe damage to the environment. Emulsion in produced water has become a major problem in oil well production ranging from cost of pumping and transportation to tainting and toxicity which can affect marine life and corrode production equipment such as pipelines [5–7].

Generally, produced water should be reused for enhanced oil recovery (EOR) or discharged into the environment after treatment. But, the oily emulsion makes it difficult to treat using conventional methods such as settling [8], centrifugation [9], coagulation and flocculation [10], flotation [11], electric methods [12,13], filtration and coalescence [14], vacuum evaporation [15,16] and membrane process [17–19]. Ultrafiltration has been proven to be very effective in the treatment of complex oily wastewater [6,20,21], since no chemical additives are required. As such the cost is lower and the low chemical oxygen demand makes the quality of the permeate obtain to be high [6]. But ultrafiltration has its limitations, the main limits are concentration polarization resulting to permeate flux decline with time.

* Corresponding author at: Department of Petroleum Engineering, School of Chemical and Energy Engineering, Faculty of Engineering, Universiti Teknologi Malaysia, 81310 Johor Bahru, Malaysia.
E-mail address: r-razuan@utm.my (R. Junin).

https://doi.org/10.1016/j.ultsonch.2018.10.023
Received 15 March 2018; Received in revised form 13 October 2018; Accepted 15 October 2018
Available online 16 October 2018
1350-4177/

Adsorption and accumulation of oil and particles on the membrane surface which causes fouling of the membrane [20,21]. Fouling shortens the membrane life span, due to frequent chemical and physical cleaning [22]. Therefore, ultrasonic is one of the most effective cleaning methods for ultrafiltration membranes [23,24].

Several researchers have used ultrasonic application in enhancing membrane filtration performance and effective cleaning of the fouled membrane. Matsumoto et al. [25] used model suspension to prevent membrane fouling, cross-flow microfiltration with ultrasonic wave cleaning. The steady-state flux obtained in filtration with ultrasonic wave was 4–6 times greater than that without ultrasonic wave, and a high flux was obtained even at a low feed velocity. Kyllonen et al. [26] focused on the effect of the ultrasound propagation direction and frequency as well as the transmembrane pressure, using on-line cleaning for the membrane filtration. It was observed that ultrasonic field produced by the transducer was uneven in pressurised conditions. Whereas, the ultrasonic treatment at atmospheric pressure during an intermission pause in filtration turned out to be efficient, and a gentler method in membrane cleaning. Various frequencies (37, 80 Hz and tandem) and sonication mode (continuous, pulsed, sweeping and degassing) using a flat-sheet membrane in cross-flow ultrafiltration was investigated by Shahraki et al. [27]. They concluded that to obtain a high permeation flux and fouling percentage, the filtration process should be performed at a low frequency and pulsed radiation mode. This was also reported by Naddeo et al. [28] when they studied the performance of sonochemical oxidation and membrane filtration of ultrasonically assisted ultrafiltration at various frequencies. They agreed with Shahraki et al. [27] that low frequency can slow down the fouling formation, but higher frequency can improve the organic matter removal. In-situ cleaning using ultrasound cavitation on the other hand, allows cleaning while filtration is still in operation. There is no need for a pause or pulsed mode as this method can reduce the cost of membrane cleaning [29]. Therefore, the combination of ultrasonic with membrane ultrafiltration can reduce membrane fouling rate at higher membrane flux and lower frequency [22].

However, Chakrabarty et al. [3] synthesized polysulfone membrane using different additives and solvents to evaluate their performance in treating oil in water emulsion. They showed that the increase in cross-flow rate, the flux increases significantly. But, the oil rejection showed a decreasing trend less than 80% which was not up to the acceptable limit of 90% rejection rate. They suggested that the membranes need further modifications to improve their properties such as pore size and pore size distribution. To tackle the difficulty of lower oil separation due to penetration of smaller oil droplets along with the permeate. A selection of appropriate membrane material, module design, operational and processing condition is needed to achieve most economical process. Therefore, the design of a successful cross-flow filtration system relies on choosing the right membrane geometry that can be used economically and provides consistent predictable results. In this study, the application of synthesized hollow and flat-sheet polyurethane (PU) membrane for oil-in-water emulsion separation is presented. The membrane performance and the characterisation of ultrasonic assisted cross-flow ultrafiltration module built to avoid loss of ultrasonic to the surrounding were applied to oil-in-water emulsions. The steady-state permeate flux and the rejection of oil in percentage (%) at two different modes were determined.

2. Materials and methods

2.1. Materials

The PU was fabricated at Advanced Membrane Technology Research Centre (AMTEC), Universiti Teknologi Malaysia. Polyethersulfone (PES) with molecular weight 4500 g/mol was supplied by Solvay Advanced Polymer, USA. Polyvinylpyrrolidone (PVP) with molecular weight 360,000 g/mol and N, N-Dimethylacetamide (DMAc) with molecular weight 87.12 g/mol and purity ≥99% were supplied by Sigma Aldrich, USA. Tween 20 with molecular weight of 1228 mol wt and a purity of 99% was supplied by Sigma Aldrich, USA. Sodium Chloride (NaCl) used in the preparation of the different brine solution was supplied by Acros Organic Company with molecular weight of 58.44 g/mol and a purity of 99% assay. Liquid paraffin which represents moderate viscosity oil was used as a substitute to crude oil.

Table 1
Composition of each component in the dope solution.

Samples	PES (wt %)	PVP (wt %)	PU (wt %)	DMAc (wt %)	Dope Viscosity (mPa·s)
1	18	3	0	78	1301.0
2	18	3	1	77	1272.8
3	18	3	2	76	1262.0
4	18	3	3	75	1246.0
5	18	3	4	74	1169.0
6	18	3	5	73	1127.3

2.2. Methods

2.2.1. Preparation of PES membrane incorporated with PU

The different weight percentage of PU were incorporated with the same weight percentage of PES and PVP. The PVP acted as the forming agent. The PES pellet was dried in the oven at 50 °C for 24 h to remove moisture prior to the dope solution preparation. PES was dissolved in DMAc solution for few hours prior to adding the PVP. Once the PES and PVP were completely dissolved, PU was added to the solution and stirred to ensure the polymers blended homogenously. Table 1 shows the composition of each component in the dope solution.

2.2.2. Hollow fibre membrane fabrication

The hollow fibre was fabricated using the same composition shown in Table 1. The PU was synthesized by polymerization and sulphonation to have an anionic group (–OH; –COOH; and $–SO_3H$) on the membrane surface. A dry/wet spinning technique was used to fabricate the PES/PVP/PU hollow fibre membrane (HFMs) with pore size 0.05 µm. A temperature of 27 °C and pressure 1–5 bar were used. This is to determine the desired structure of the membrane [30]. The spinning parameter for the PES/PVP/PU composite HFMs fabrication was based on the result obtained in the study of the suitable spinning parameters. The PES/PU HFMs was compared with PES/PVP HFMs in terms of their morphology and characteristics. The spinning parameters for the hollow fibre membranes fabrication are shown in Table 2.

2.2.3. Flat-sheet membrane fabrication

The flat-sheet membrane was fabricated using the same composition shown in Table 1. The polymer dope solution prepared was poured on a flat glass plate of dimension (300 mm × 200 mm × 3 mm). A glass rod of length (300 mm) and diameter (18 mm) was used to spread the

Table 2
Spinning parameter for HFMs fabrication.

Air Gap (cm)	50
Dope Prepared (ml)	200
DER (cm^3/min)	1
DER (rpm)	3.33
BFFR (cm^3/min)	1
LER (cm/s)	7.86
CD Speed (s/rev)	6.98
CD Value (Hz)	4.0
CD (m/min)	10
Min/100 m	10
Coagulated Bath	Tap Water
Coagulated Bath Temperature	Room Temperature
Bore Fluid	Distilled Water

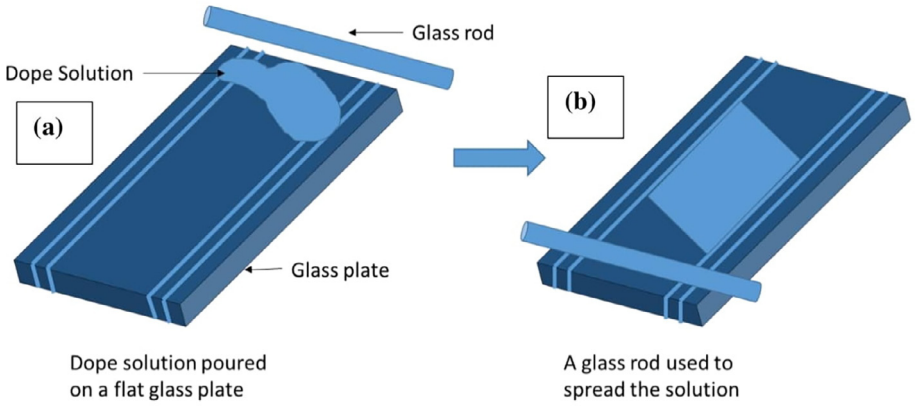

Fig. 1. (a) Glass plate and rod with doped solution before spreading, (b) Glass plate and rod with doped solution after spreading.

solution to a uniform thickness by applying a layer of masking tape at both edges of the glass plate as shown in Fig. 1. The glass plate was then immersed in the coagulation bath. This is to enable precipitation of the membrane film as exchange between the solvent and non-solvent take place. The water was used as the coagulant at room temperature. The film detached from the glass plate after solidification and was immersed in water for 24 h before drying for another 24 h.

2.2.4. Emulsion samples preparation

The oil-in-water emulsion was prepared by mixing 0.94 wt% of brine with 1.1 wt% of surfactant to act as the emulsifying agent. 1000 ml of paraffin was slowly added to the mixture at a constant rate of agitation (2000 rpm). The salinity concentration was chosen to depict a typical Malay Basin oilfield salinity which varies between 9000 and 22,000 ppm. The salinity also correlates between the oilfield brine and interfacial tension (IFT), which is the lowest IFT to form a stable emulsion [31]. Low IFT as well as small droplet were obtained from the stable emulsion. The emulsion created turned to milky white in colour after agitating for 6 h. The properties of the simulated O/W emulsion are shown in Table 3.

2.3. Ultrafiltration experiment

2.3.1. Ultrasonic module

An ultrasonic generator provided the energy which was emitted to a water bath through an immiscible transducer. A Crest Genesis™ XG-500-6 ultrasonic generator with a frequency of 40 kHz and power output of 500 W provided the ultrasound. The cross-flow ultrafiltration filter was installed inside a stainless-steel cartridge housing filled with deionized water and immersed totally in an ultrasonic bath. The bath (W: 21 cm × L: 50 cm x H: 30 cm) was designed to make a suitable surrounding for the application of the ultrasound.

2.3.2. Cross-flow filtration membrane and ultrasonic

The experiments were performed at 2 bars using a cross-flow ultrafiltration system (Fig. 2) containing polymeric ultrafiltration membrane immersed in ultrasonic water bath. Deionized water was injected into the system to evacuate any impurities and allow the permeate flux to stabilize. O/W emulsion was placed in a feed tank and heated for 30 min as a pre-treatment to the emulsion. The permeate side was then open to the atmosphere. The permeate was collected in a beaker and the permeate flux was acquired by the volume of the permeate at a certain time. The membrane was returned to the feed tank after 25 min of the filtration process. The membrane undergoes cleaning for another 10 min. During the membrane cleaning, the filtration process is stopped allowing clean water to pass through the membrane. Hence, the oil retentate can be flushed out of the membrane. The experiment was conducted for filtration process without ultrasonic and with continuous ultrasonic and constant power. The permeate flux, J was calculated;

$$J = \frac{V}{A\Delta t} \tag{1}$$

whereas J is the permeate flux (L/m^2h), V is the volume of permeate collected (L), A is the membrane area (m^2), and Δt is the permeation time (h).

The separation efficiency or oil rejection efficiency (R_o) of the filter is the ability to retain dispersed oil phase from flowing across the filter surface;

$$R_o = \left(1 - \frac{C_p}{C_f}\right) \times 100\% \tag{2}$$

whereas C_p and C_f are the measured oil concentration of the permeate and feed respectively. The rejection ratios (R_o) of the oil were calculated by determining the oil concentration in the feed and permeate solutions using UV-spectrophotometer.

The flux declination can be obtained from the initial influx as;

$$\textit{flux delination} = \left(1 - \frac{J_t}{J_i} \times 100\%\right) \tag{3}$$

whereas J_t is the permeate flux at a certain time, and J_i is the initial flux.

Table 3
Properties of simulated O/W emulsion.

Parameters	Values
Interfacial Tension (mNm)	34.60
Viscosity (mPa·s)	6.872
pH	6.5
Water Salinity (%)	0.94
Oil Concentration (ppm)	1000

2.3.3. Oil concentration determination using UV-spectrophotometer

The UV-spectrophotometer was used to determine the concentration of oil in the synthetic emulsion. It measures the attenuation of the beam of light that passes through a sample or after reflection from a sample surface. The adsorption measurement can be a single wavelength or over an extended spectral range. Six emulsion samples with different percentage oil ranges (0–50%) were used to construct a calibration curve. The percentage of oil in the permeate was determined from the calibration curve. The rejection ratio was calculated using Eq. (2).

3. Results and discussion

3.1. Morphology of composite PES/PVP/PU membranes

The SEM image of the membrane module is shown in Fig. 3

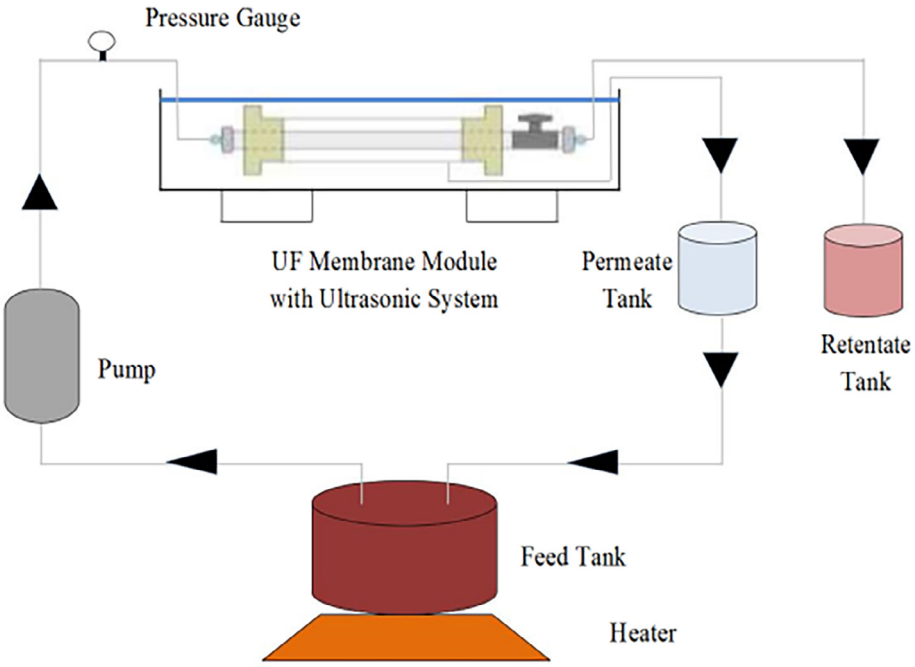

Fig. 2. Schematic representation of ultrafiltration membrane and ultrasonic process.

whereas, the cross-section and surface of the composite HFMs are shown in Figs. 4 and 5 respectively. The cross-section shows that the outer diameter ranges from 369 μm to 398 μm. Whereas, the inner diameter ranges from 266 μm to 283 μm, each of the membrane has a dense area in the inner surface near the lumen and a finger-like structure near the end of the outer membrane (Fig. 6). The finger-like structure near the edge of the outer membrane eased the movement of the emulsion during cross-flow and prevented back flow to occur. The finger-like porous structure might be responsible for the mechanical strength of the whole structure, thereby preventing the HFMs from collapsing [32]. The porous membrane matrix can promote coalescence of micron and submicron oil droplet into larger ones that can be easily separated by gravity [33]. The membrane was denser near the inner surface and the skin layer acted as a selective layer in retaining and releasing of the retentate and permeate.

The asymmetric, microporous ultrafiltration hollow-fibre was successfully produced for each different composition of the membrane as shown in Fig. 6. Similar result was also observed by Kumar et al. [4]. The formation of the asymmetry structure is due to the manipulation of the spinning parameters [34]. Also, the high mutual affinity of PES to water resulted in instantaneous demixing might be responsible [4]. The air gap of 50 cm was used during the spinning inversion process. The high air gap distance gave additional stretching to the membrane, consequently reducing the fibre dimension (200–300 μm). Also, the solvent/non-solvent exchange during the phase inversion process could have determined the structure of the membrane. Longer dry phase inversion prolonged the solvent (DMAc) and the non-solvent (water) demixing process. Resulting in the fast phase separation at the outer skin and slow phase separation at the inner layer [35].

As the concentration of PU in the membrane increased, the finger-like pore structure became more porous. Also, from the SEM images of the surface morphology for each membrane with different PU concentration (Fig. 4), the PES/PVP membrane without any PU added has a typical pore size range from 40 to 60 nm. In contrast, the pore size of the membrane decreased and was uniformly distributed as more PU (1–3 wt%) was added. Similar result was observed by Kumar et al. [4] however, as more PU was added (4–5 wt%), the pore size increased. This could be because of the viscosity of the dope solution and the fabricated membrane during phase inversion. The viscosity of the dope might have affected the time taken for the solvent/non-solvent exchange during phase inversion. As the concentration of PU added to the dope solution increased, the viscosity of the dope was decreased. Similar result was also reported by Ismail et al. [36] when they reported that low viscosity of dope solution can fasten the exchange rate of

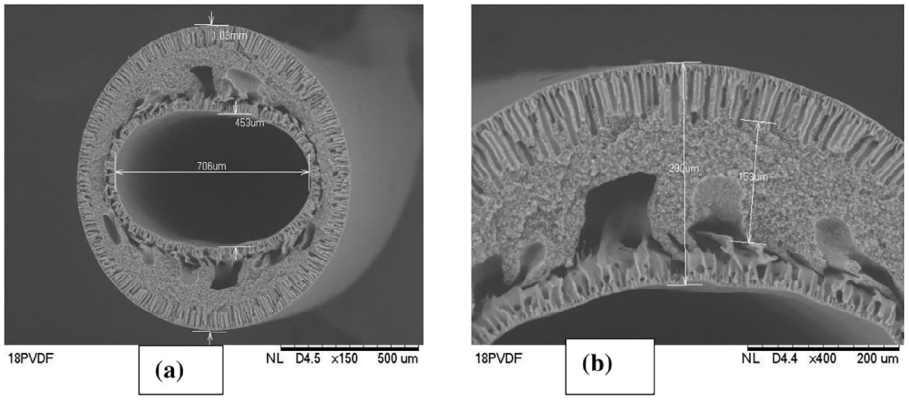

Fig. 3. SEM image of HFMs.

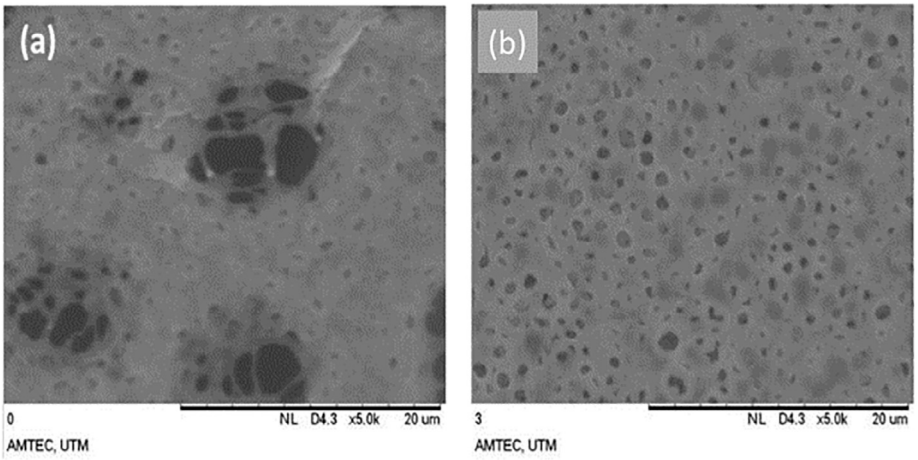

Fig. 4. SEM image of hollow fibre membrane spun from 0 to 5% of PU surface at different magnification. (a) PES/PVP, and (b) PES/PVP/PU3%; magnification 5000×.

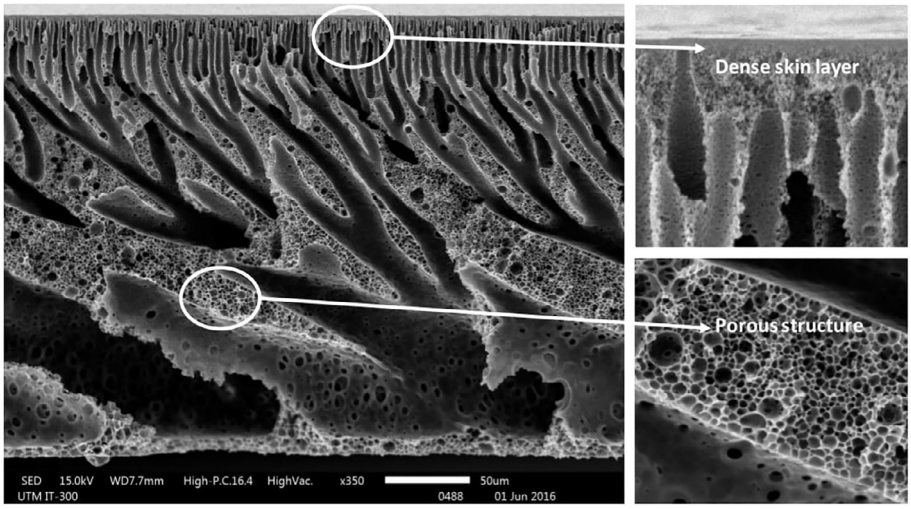

Fig. 5. SEM Image of PES/PVP/PU4%.

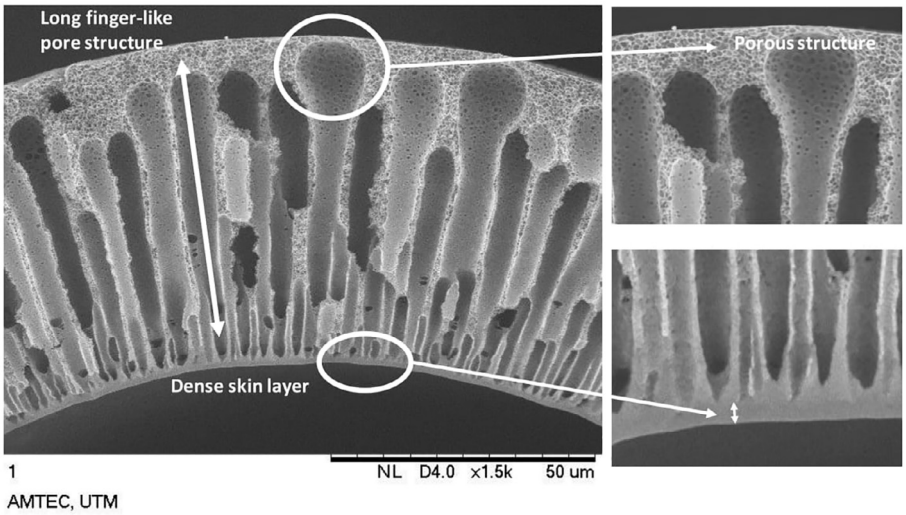

Fig. 6. SEM image of PES/PVP/PU4%, showing dense skin layer and finger-like structure.

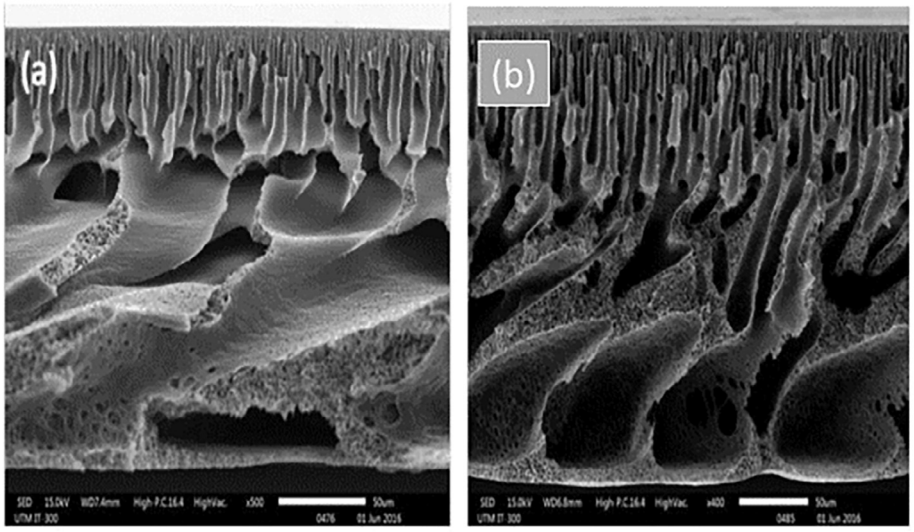

Fig. 7. SEM image of flat-sheet membrane spun from 0 to 5 wt% of PU cross-sectional region at different magnification (a) PES/PVP (b) PES/PVP/PU 3 wt%.

solvent.

Figs. 7 and 8 show the SEM images for the cross-sectional and surface morphology of the composite flat-sheet membrane. The flat sheet membrane has a dense skin layer near the inner surface of the membrane and porous finger-like structure close to the edge of the membrane. A wave-like porous finger-like structure was formed close to the edge of the membrane (Fig. 7). The result for the composite flat-sheet membrane corresponds to the composite hollow fibre. As the concentration of PU increased, the finger-like pore structure became porous. The surface morphology of the flat-sheet membrane showed the same pattern of pore size increment, where the pore size increased as the concentration of PU increased [37,38].

3.2. Permeate flux without ultrasonic

The experiment without ultrasonic was conducted at room temperature, the membrane was cleaned twice without ultrasonic for 10 min each. Fig. 9 shows the permeate flux filtration without ultrasonic. As the filtration time increased, the permeation flux decreased from 40.23 to 32.18 L/m^{2}h. The permeate flux decline after 15 min of filtration (Fig. 9). Similar result was observed by Sablani et al. [39] and Kumar et al. [4] when they reported adsorption of particles at the membrane pores causing blocking after 10 min filtration [3]. This decline of the permeate flux could be due to the resistance of the membrane surface. Due to the compact nature of the fouling layer of the filtration without ultrasonic [40]. The longer the filtration process, the increase in resistance at the membrane surface, whereas the resistance is proportional to the filtration time. Also, the membrane fouling became severe because of the cake formed at the surface. The adsorption of the particles on the membrane pores and concentration polarization which is caused by the permeate flux, will cause particles to deposit on the membrane surface [3,4]. The flux approached a steady state condition during the last minutes of the filtration. This is in line with previous study by Chakrabarty et al. [3] when they reported that the permeate flux of membranes decreases with time and approaches a steady state after a certain duration of time. Theoretically, when the convention flow towards the membrane and the permeate flow passing through, the membrane achieve equilibrium condition, the permeate flux is in steady state [41]. The formation of cake layer around the membrane surface prevented the flux from going through the membrane walls thus decreasing the flux. The permeate flux pattern also decreased slowly, this is due to the oil droplet blocking the pores [3,4].

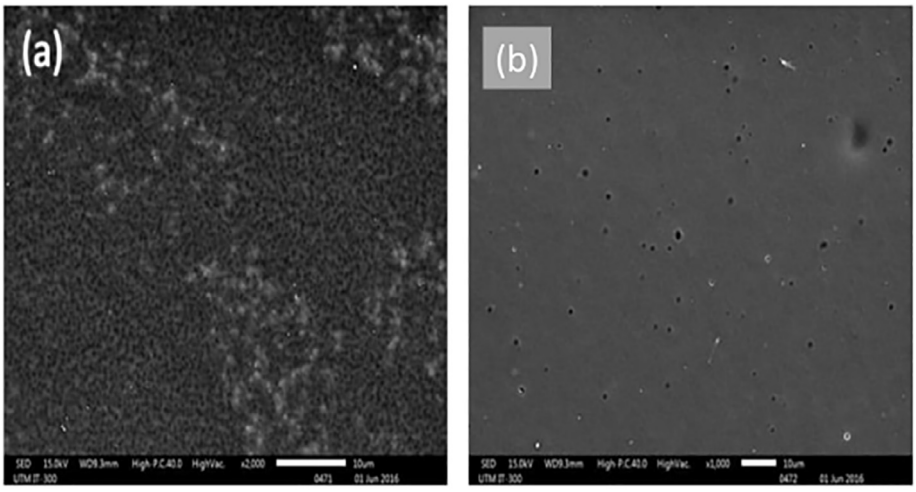

Fig. 8. SEM image of flat fibre membrane spun from 0 to 5 wt% of PU surface at different magnification (a) PES/PVP, and (b) PES/PVP/PU 3 wt% magnification 2000×.

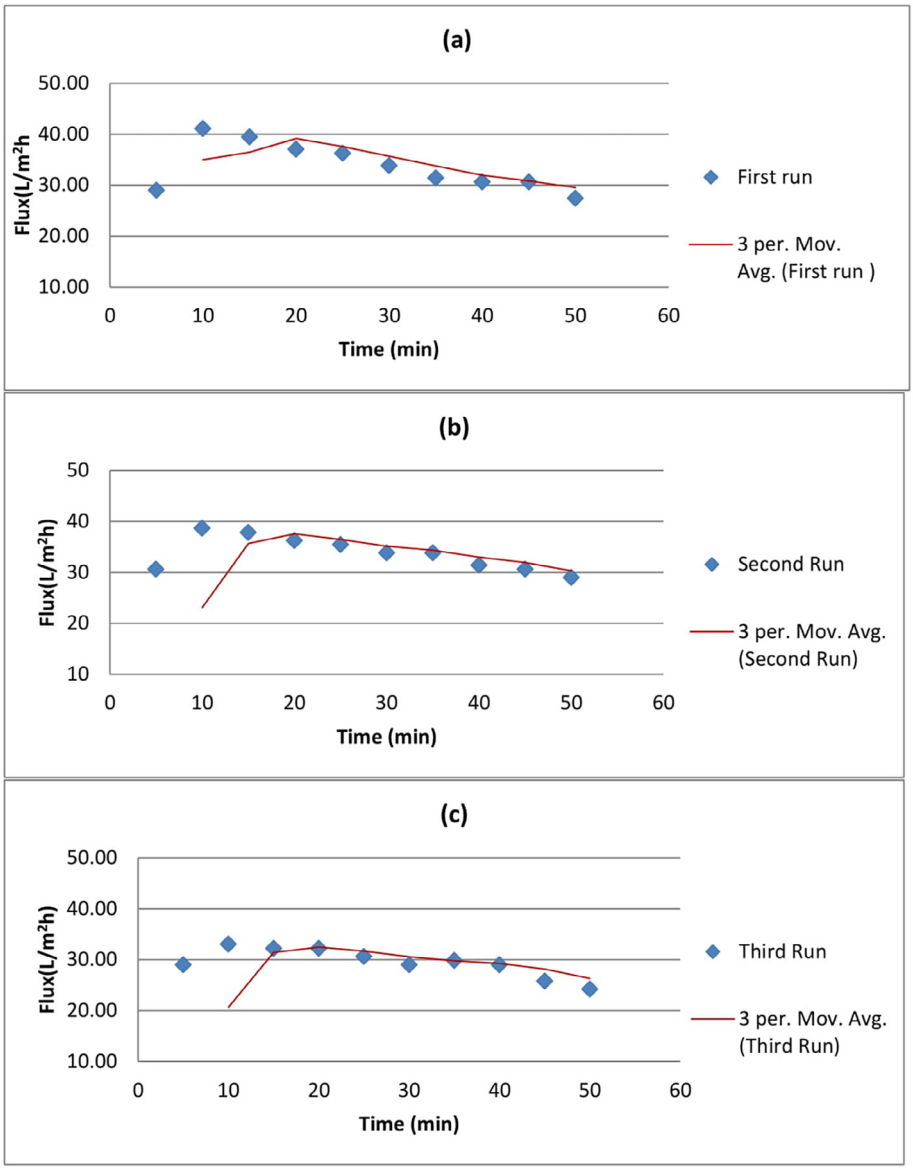

Fig. 9. Permeate flux filtration without ultrasonic (The red lines show 3 points moving average trendline) (a) First filtration process, (b) Second filtration process after first membrane cleaning, and (c) Third filtration process after second membrane cleaning. (For interpretation of the references to colour in this figure legend, the reader is referred to the web version of this article.)

3.3. Permeate flux with continuous ultrasonic and constant power

Fig. 10 shows the changes in the permeate flux with operating time carried out with ultrasonic. When the ultrafiltration was carried out, the permeate flux initially decreased rapidly and reached a steady state (Fig. 10a). After the second and third membrane cleaning by ultrasonic (Fig. 10b and c), the permeate flux improved and became higher but with slight declination compared to the first filtration (Fig. 10a) and without ultrasonic (Fig. 9). This is because the continuous use of ultrasonic has a high cleaning efficiency which is very effective in removing the cake layer formed on the membrane surface [25,42]. The increase in the flux is because the ultrasonic dislodged more tightly bound material at the surface. The membrane surface shows flocculation with ultrasonic, the flocculating fouling resistance was less compared to that of the compact fouling layer without ultrasonic. Which led to the high permeate flux, the ultrasonic-assisted filtration changed the morphology of the membrane fouling surface. Resulting in reduced adhesion strength between the fouling layer and membrane surface [40]. The mechanism responsible for this is cavitation during the ultrasonication that caused the cake to be physically disrupted. This agrees with previous studies by Kobayashi et al. [43] when they reported the enhanced permeability during sonication between individual protein and lactose molecules, further enhanced the cleaning effect. Ultrasonic can be used to separate physical aggregation of such molecules by disrupting the intermolecular forces. Cavity bubbles grow during long rarefaction cycle of sonic waves [44]. The number of cavitation bubbles increase with size [26] and the cleaning effect could increase due to turbulence [27]. The cleaning of the particles adhered to the surface is achieved by shear forces which are available by oscillating the bubble cavitation near the wall. The generated cavitation by ultrasonic cracked the cake layer and help the gas bubble to detach from the membrane surface. In these mechanisms, the fluid is sucked and ejected away from the bubble and from the wall in a sweeping mode [45]. As such concentration polarization is reduced leading to improved ultrafiltration flux. Also, acoustic streaming and shock waves produced by the ultrasonic might set the particles in motions (Brownian motion), thereby dislodging them from the membrane surface and preventing deposition of the particles that results in membrane fouling

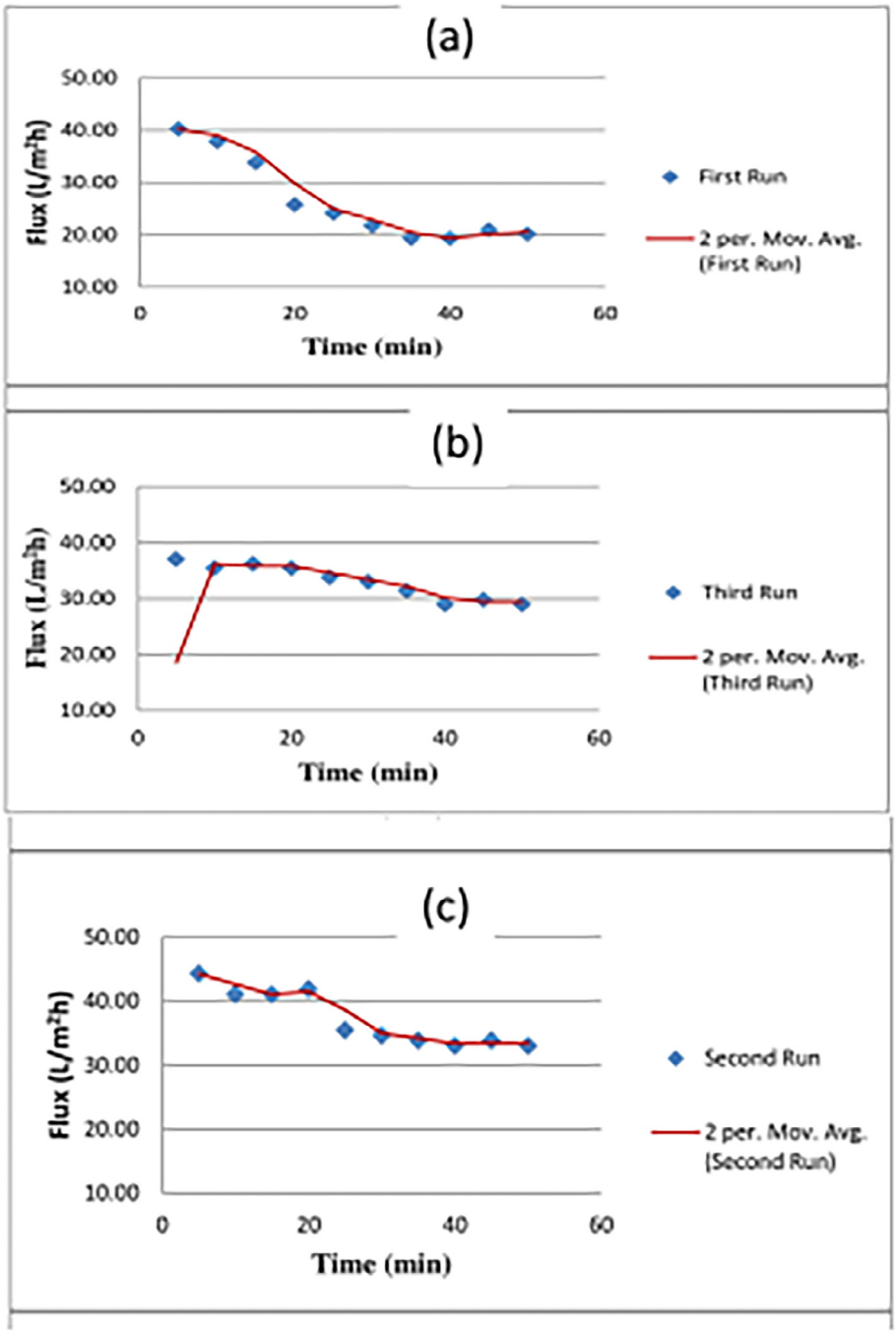

Fig. 10. Permeate flux with ultrasonic (40 KHz; 200 Watts) (The red lines show 2 points moving average trendline) (a) First filtration process, (b) Second filtration process after first membrane cleaning, and (c) Third filtration process after second membrane cleaning. (For interpretation of the references to colour in this figure legend, the reader is referred to the web version of this article.)

Table 4
Percentage of oil after ultrafiltration process.

Condition/Parameters	Adsorption	Oil Volume (%)	Rejection Ratio (%)
Continuous Ultrasonic	0.225	0.5	90
Without Ultrasonic	0.400	1.2	49

[46–49].

3.4. Oil concentration in the permeates

The ultrafiltration with continuous ultrasonic was the most significant result with a small amount of residual oil and high amount of oil rejected. Whereas, the amount of residual oil for ultrafiltration without ultrasonic was relatively high (Table 4). The percentage of oil after ultrafiltration process with ultrasonic is about 90% whereas, without ultrasonic is about 49%. These results show that ultrasonic waves can enhance the process of ultrafiltration and increase its effectiveness. Ultrasonic is effective in enhancing the membrane permeate flux and controlling membrane fouling.

4. Conclusions

The performance of ultrafiltration flow for the treatment of polluted

oil-in-water emulsion to fulfil the regulatory requirements for purified effluent in the sea was evaluated. After performing laboratory experiments, analysing data and discussing the results, the following conclusions were made:

(a) The pore size of the membrane increased as the concentration of the PU increased for both hollow and flat-sheet membranes.
(b) The formation of finger-like structure close to the edge of the membrane eased the movement of the emulsion during cross-low and prevented back flow. The finger-like structure was also responsible for the mechanical strength of the structure.
(c) Ultrasonic assisted cleaning of membrane can improve the quality of the filtration process and enhance the quantity of permeate thus, increasing the flux through the membrane pores.
(d) The generation of cavitation and Brownian motion by the ultrasonic were the dominant mechanisms responsible for ultrafiltration by cracking the cake layers and reducing concentration polarization at the membrane surface.

Acknowledgements

The authors would like to thank the Ministry of Higher Education (MOHE), Malaysia and Universiti Teknologi Malaysia for supporting this research through Research Management Grant Vot. No. R. J130000.7846.4F946 and UTM-TDR43.1.

References

[1] K.S. Ashaghi, M. Ebrahimi, P. Czermak, Ceramic ultra and nanofiltration membranes for oil field produced water treatment: a mini review, Open Environ. Sci. 1 (2007) 1–8.
[2] R. Lee, R. Seright, M. Hightower, M. Cather, B. McPherson, L. Wrotenbery, D. Martin, M. Whitworth, Strategies for Produced Water Handling in New Mexico, in: presented at the Ground Water Protection Council Produced Water Conference held in Colorado Springs Co; USA, 2002, pp. 16–17.
[3] B. Chakrabarty, A.K. Ghoshal, M.K. Purkait, Cross-flow ultrafiltration of stable oil-in- water emulsion using polysulfone membrane, Chem. Eng. J. 165 (2010) 447–456.
[4] S. Kumar, B.K. Nandi, C. Guria, A. Mandal, Oil removal from produced water by ultrafiltration using polysulfone membrane, Braz. J. Chem. Eng. 34 (2) (2017) 583–596.
[5] A. Zaidi, K. Simms, S. Kok, The use of micro/ultrafiltration for removal oil and suspended solids from oil field brines, Water Sci. Technol. 25 (10) (1992) 163–176.
[6] D. Allende, D. Pando, M. Matos, C. Carleos, C. Pazos, J. Benito, Optimization of membrane hybrid process for oil-in-water emulsion treatment using taguchi experimental design, Desalin. Water Treat. (2015) 1–10.
[7] A. Agi, R. Junin, M.I. Zakariah, T.B. Bukkapattanam, Effect of temperature and acid concentration on Rhizophora mucronate tannin as a corrosion inhibitor, J. Bio Tribo-Corros. 4 (5) (2018) 1–10.
[8] M. Simmons, E. Komonibo, B. Azzopardi, D. Dick, Resistance time distribution and flow within primary crude oil- water separators treating well head fluids, Ind. Eng. Chem. Res. 82 (2004) 1383–1390.
[9] D. Allende, A. Cambiella, J.M. Benito, C. Pazos, J. Coca, Destabilization-enhanced configuration of metalworking oil-in-water emulsion: effect of demulsifying agents, Chem. Eng. Technol. 31 (2008) 1007–1014.
[10] J.L. Kenneth, Demulsification: Industrial Applications, Marcel Dekker, New York, USA, 1983.
[11] D. Tao, Role of bubble size in flotation of coarse and fine particles - a review, Sep. Sci. Technol. 39 (2004) 741–760.
[12] P. Canizares, F. Martinez, E. Jimenez, C. Saez, M.A. Rodrigo, Coagulation and electrocoagulation of oil-in-water emulsion, J. Hazard. Mater. 151 (2008) 44–51.
[13] M. Emamjomeh, M. Sivakumar, Review of pollutants removed by electrocaogulation and lectrocoagulation/filtration process, J. Environ. Manage. 90 (2009) 1663–1679.
[14] R.S. Sokolovic, S. Sokolovic, S. Sevic, Oily water treatment using a steady-state fibre-bed coaleser, J. Hazard. Mater 162 (2009) 410–415.
[15] G. Guetierrez, A. Cambiella, J.M. Benito, C. Pazos, J. Coca, Effect of additives on treatment of oil-in-water emulsion by vacuum evaporation, J. Hazard. Mater. 144 (2007) 649–654.
[16] G. Guetierrez, J.M. Benito, J. Coca, C. Pazos, Vacuum evaporation of surfactant solutions and oil-in-water emulsion, Chem. Eng. J. 162 (2010) 201–207.
[17] V. Singh, M.K. Purkait, C. Das, Cross-flow microfiltration of industrial oily waste water: experimental and theoretical consideration, Sep. Sci. Technol. 46 (2011) 1213–1223.
[18] D. Vasanth, G. Pugazhenthi, R. Uppaluri, Cross-flow microfiltration of oil-in-water using low cost ceramic membranes, Desalination 320 (2013) 86–95.
[19] Q.B. Chang, J.E. Zhou, Y.Q. Wang, J. Liang, X.Z. Zhang, S. Cerneaux, X. Wang, Z.W. Zhu, Y.C. Dong, Application of ceramic nanofiltration membrane modified by nano-TiO_2 coating in separation of a stable oil-in-water emulsion, J. Membr. Sci. 456 (2014) 128–133.
[20] A. Lobo, A. Cambiella, J.M. Benito, C. Pazos, J. Coca, Ultrafiltration of oil-in-water emulsions with ceramic membranes: influence of pH and crossflow velocity, J. Membr. Sci. 278 (2005) 328–334.
[21] G.N. Vatai, D.M. Krstic, A.K. Koris, I.L. Gaspar, M.N. Tekic, Ultrafiltration of oil-in-water emulsion: comparison of ceramic and polymeric membrane, Desalin. Water Treat. 3 (2009) 162–1168.
[22] L. Borea, V. Naddeo, M.S. Shalaby, T. Zarra, V. Belgiomo, H. Abdalla, A.M. Shaban, Wastewater treatment by membrane ultrafiltration enhanced with ultrasound: effect of membrane flux and ultrasonic frequency, Ultrasonic 83 (2018) 42–47.
[23] R. Deqian, Cleaning and regeneration of membranes, Desalination 62 (1987) 363–371.
[24] S. Muthukumaran, S. Kentish, S. Lalchandani, M. Ashokkumar, R. Mawson, G.W. Stevens, F. Grieser, The optimization of ultrasonic cleaning procedures for dairy fouled ultrafiltration membrane, Ultrason. Sonochem. 12 (2005) 29–35.
[25] Y. Matsumoto, T. Miwa, S. Nakao, S. Kimura, Improvement of membrane permeation performance by ultrasonic microfiltration, J. Chem. Eng. Jpn. 29 (4) (1996) 561–567.
[26] H. Kyllonen, P. Pirkonen, M. Mystrom, Membrane filtration enhanced by ultrasound: a review, Desalination 181 (2005) 319–335.
[27] M.H. Shahraki, A. Maskooki, A. Faezian, Effect of various sonication mode on permeation flux in cross flow ultrafiltration membrane, J. Environ. Chem. Eng. 2 (4) (2014) 2289–2294.
[28] V. Naddeo, L. Borea, V. Belgiorno, Sonochemical control of fouling formation in membrane ultrafiltration of wastewater: effect of ultrasonic frequency, J. Water Process Eng. 8 (2015) 92–97.
[29] W.L. Loh, T.T. Wan, V.K. Premanadham, K.K. Naing, N.D. Tam, V.H. Perez, Y. Qiao, Z. Wang, Z. Wang, Experimental study of separation of oil in water emulsions by tangential flow microfiltration process part 2: the use of ultrasound for in-situ controlling of membrane fouling, Membr. Sci. Technol. 5 (1) (2014) 1–5.
[30] C.F. Wan, T. Yang, G.G. Lipscomb, D.J. Stookey, T.S. Chung, Design and fabrication of hollow fiber membrane modules, J. Membr. Sci. 538 (2017) 96–107.
[31] A. Zulkania, B. Pramudono, H.B. Mat, A.K. Idris, M.A. Manan, Malaysian Crude Oil Emulsions: Physical and Chemical Characterization, in: 15th Symposium of Malaysian Chemical Engineers SOMChE, E1-1, 2001, pp. 435–442.
[32] X. Xu, L. Heng, X. Zhao, J. Ma, J. Lin, L. Jiang, Multiscale bio-inspired honeycomb structure material with high mechanical strength and low density, J. Mater. Chem. 21 (22) (2012) 10883–10888.
[33] M. Hlavacek, Breakup of oil-in-water emulsion induced by permeation through microfiltration membrane, J. Membr. Sci. 102 (1995) 1–7.
[34] A. Manchon, H.C. Koo, J. Nitta, S.M. Frosolov, R.A. Duine, New Spinning perspectives for Rashba spin-orbit coupling, Nat. Mater. 14 (2015) 871–882.
[35] N. Hilal, A.F. Ismail, C.J. Wright, Membrane Fabrication, CRC Press, Taylor and Francis Group, Florida, USA, 2015.
[36] A.F. Ismail, M.I. Mustaffar, R.M. Illias, M.S. Abdullah, Effect of dope extrusion rate on morphology and performance of hollow fibre membrane for ultrafiltration, Sep. Purif. Technol. 49 (1) (2006) 10–19.
[37] S.H. Neubert, Controllability of electrospinning and electrospraying-advances and application, M.Eng Thesis National University of Singapore, 2010.
[38] W. Teo, R. Inai, S. Ramakrishna, Technological advances in electrospinning of nanofibres, Sci. Technol. Adv. Mater 12 (2011) 1–19.
[39] S.S. Sablani, M.F. Goosen, R. Al-Belushi, M. Wilf, Concentration polarization in ultrafiltration and reverse osmosis, a critical review, Desalination 141 (2001) 269–289.
[40] S. Li, X. Weihong, X. Nanping, Effect of ultrasound on the treatment of emulsion waste water by ceramic membranes, Chin. J. Chem. Eng. 15 (6) (2007) 855–860.
[41] M. Cheryan, N. Rajagopalan, Membrane processing of oily streams. waste water treatment and waste reduction, J. Membr. Sci. 151 (1) (1998) 13–28.
[42] M.H. Shahraki, A. Maskooki, A. Faezian, A. Rafe, Flux improvement of ultrafiltration membranes using ultrasound and gas bubbling, Desalin. Water Treat. (2016) 1–10.
[43] T. Kobayashu, X. Chain, N. Fujii, Ultrasound enhanced cross-flow membrane filtration, Sep. Purif. Technol. 17 (1999) 31–40.
[44] T. Kobayashi, T. Kobayashi, Y. Hosaka, N. Fujii, Ultrasound-enhanced membrane process applied water treatments: influence of sonic frequency on filtration treatments, Ultrasonic 41 (2003) 185–190.
[45] M. Marmottant, M. Versluis, N. De Jong, S. Hilgenfeldt, D. Lohse, High speed imaging of an ultrasound-driven bubble in contact with a wall: “Narcissus” effect and resolved acoustic streaming, Exp. Fluids 41 (2006) 147–153.
[46] D. Chen, L.K. Weavers, H.W. Walker, Ultrasonic control of ceramic membrane fouling: effect of particles characteristics, Water Res. 40 (2006) 840–850.
[47] A. Agi, R. Junin, M. Shirazi, A. Gbadamosi, N. Yekeen, Comparative study of ultrasound assisted surfactant and water flooding, J. King Saud Univ.-Eng. Sci. (2018).
[48] A. Agi, R. Junin, A. Yahya, A. Gbadamosi, A. Abbas, Comparative study of continuous and intermittent ultrasonic ultrafiltration membrane for the treatment of synthetic produced water containing emulsion, Chem. Eng. Process. Process Intensif. 132 (2018) 137–147.
[49] A. Agi, R. Junin, A.S. Chong, Intermittent ultrasonic wave to improve oil recovery, J. Petrol. Sci. Eng. 166 (2018) 577–591.